THE JOURNAL OF PHYSICAL CHEMISTRY B

Article

pubs.acs.org/JPCB

Excited State Structure and Dynamics of the Neutral and Anionic Flavin Radical Revealed by Ultrafast Transient Mid-IR to Visible Spectroscopy

Andras Lukacs,[†,⊥] Rui-Kun Zhao,[†] Allison Haigney,[‡] Richard Brust,[‡] Gregory M. Greetham,[§] Michael Towrie,[§] Peter J. Tonge,*[,‡] and Stephen R. Meech*[,†]

[†]School of Chemistry, University of East Anglia, Norwich Research Park, Norwich NR4 7TJ, United Kingdom

[‡]Department of Chemistry, Stony Brook University, Stony Brook, New York 11794-3400, United States

[§]Central Laser Facility, Research Complex at Harwell, Rutherford Appleton Laboratory, Didcot OX11 0QX, United Kingdom

[⊥]Department of Biophysics, Medical School, University of Pecs, Hungary

Supporting Information

ABSTRACT: Neutral and anionic flavin radicals are involved in numerous photochemical processes and play an essential part in forming the signaling state of various photoactive flavoproteins such as cryptochromes and BLUF domain proteins. A stable neutral radical flavin has been prepared for study in aqueous solution, and both neutral and anion radical states have been stabilized in the proteins flavodoxin and glucose oxidase. Ultrafast transient absorption measurements were performed in the visible and mid-infrared region in order to characterize the excited state dynamics and the excited and ground state vibrational spectra and to probe the effect of the protein matrix on them. These data are compared with the results of density functional theory calculations. Excited state decay dynamics were found to be a strong function of the protein matrix. The ultrafast electron transfer quenching mechanism of the excited flavin moiety in glucose oxidase is characterized by vibrational spectroscopy. Such data will be critical in the ongoing analysis of the photocycle of photoactive flavoproteins.

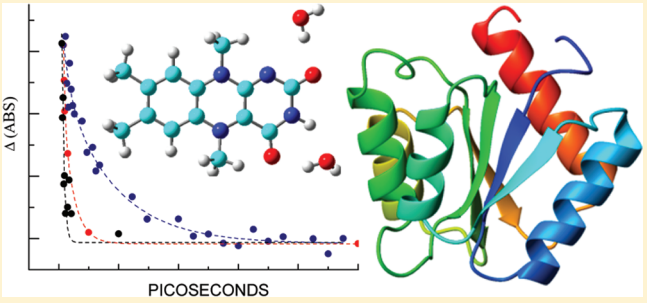

INTRODUCTION

Redox properties of flavin molecules endow flavoenzymes with huge versatility in their function. Their ability to exist in oxidized, one-electron and two-electron reduced states means that they can take part in a wide variety of redox processes.[1] Photoactive flavoenzymes are a special class of proteins where the blue light absorbing flavin cofactor plays a role in a light-activated function.[2] For example, in photolyase—a known DNA repair enzyme—the fully reduced flavin cofactor transfers an electron to the cyclobutane pyrimidine dimer lesion upon light excitation, resulting in the cleavage of the pyrimidine–pyrimidine bond. In almost all the isolated photolyase enzymes, the flavin is in its neutral radical state and a second photoprocess is required: after absorption of a visible photon, the cofactor is reduced via an electron transfer cascade mechanism involving a tryptophan chain.[3,4] Although this latter mechanism is possibly not of physiological significance, it is important in cryptochromes, another enzyme family involved in the photoregulation of the circadian rhythm and perhaps in magnetoreception in birds.[5,6]

Another important class of blue light sensing flavoproteins are the blue light using FAD (BLUF) domain family, where FAD is flavin adenine dinucleotide. The BLUF proteins are involved in the photophobic response and in light-controlled gene expression in bacteria.[2] The mechanism of photoactivity in the BLUF domain has not yet been definitively established. Detailed studies of the gene-regulating AppA protein, which contains one of the best characterized BLUF domains,[7−9] reveal a kinetically complex photocycle with a number of steps occurring on the picosecond time scale.[10,11] However, transient visible and mid-IR spectroscopy have yet to identify any intermediates between the dark-adapted state and the light-activated signaling state.[12,13] On the other hand, the PixD BLUF domain involved in phototaxis was reported to reveal an electron transfer in the photocycle where, after optical excitation, the initially oxidized flavin cofactor is reduced by a nearby tyrosine residue forming the anionic radical state and then the neutral protonated state, through a proton transfer reaction, before finally forming the signaling state.[14] The signaling state is believed to be reached after a structural and H-bond reorganization among amino acid residues near the flavin.[7,15]

Received: December 4, 2011
Revised: March 30, 2012
Published: April 19, 2012

Clearly the proper characterization of the flavin radical's ground and excited state electronic and vibrational spectroscopy and its excited state dynamics will be critical to the elucidation of the photocycle in these photoactive flavoproteins. In this work we present ultrafast transient absorption measurements in the visible and mid-infrared region performed on anionic and neutral flavin radicals, both in solution and bound to two proteins. With these methods we are able to identify specific spectroscopic signatures of potential flavin redox intermediates in various photoactive flavoproteins, and to record their formation and decay kinetics. These data are then applied to the analysis of the quenching of oxidized FAD in glucose oxidase (GOX). This work extends our earlier studies of the fully reduced and fully oxidized flavins in solution.[12,16]

MATERIALS AND METHODS

Synthesis of Model Flavin Neutral Radicals. The 5-methyl FAD radical (5-CH_3FAD$^\bullet$) and 5-methyl FMN radical (5-CH_3FMN$^\bullet$) were made by anaerobic chemical reduction following Eisenberg's method.[17] Briefly, sodium cyanoborohydride (Sigma-Aldrich) was dissolved in 1 mL of 2.2 M formaldehyde D_2O solution. Separately 10 mg of FAD (or 5 mg of FMN) and 5.6 mg of sodium dithionite were dissolved in 2 mL of 0.5 M D_2O phosphate buffer at pD 5.0. Both solutions were degassed by bubbling nitrogen gas for 30 min. The sodium dithionite reduced the FAD to $FADH_2$ (or FMN to $FMNH_2$), and the $FADH_2$ ($FMNH_2$) solution was transferred with a gas-tight syringe into the sodium cyanoborohydride/formaldehyde solution in a 4 mL glass vial sealed with a rubber septum. The solution was stirred for 1 h resulting in the formation of 5-methylated fully reduced states. The reaction is illustrated in the Supporting Information. The radical state was prepared by removing 50 μL of this stock solution and placing it in a 1 mL eppendorf and then adding 500 μL of distilled water or D_2O; after shaking the radical state was formed. Complete formation of the radical form and its concentration were determined by UV−vis spectroscopy.[18]

FADH$^\bullet$ in GOX and Flavodoxin. Glucose oxidase (GOX) from *Aspergillus niger* (Sigma) was prepared in 60 mM phosphate buffer at pH 6.0. The semiquinone was prepared in the presence of 10 mM EDTA following Massey's method in which the sample was degassed, followed by 0.5−1 h illumination with a Schott K-500 150 W halogen lamp via an optical fiber attachment.[19] Flavodoxin from *Desulfovibrio gigas* was originally stored in a 50 mM MOPS buffer, pH 7.0. Before the time-resolved IR (TRIR) measurement, the buffer was exchanged in 50 mM phosphate buffer pD 7.0, and the final concentration of the sample was ∼150 μM. The semiquinone form of flavodoxin was prepared by the same method as that described above for GOX.

Time-Resolved IR Measurements. Time-resolved infrared measurements (TRIR) were performed using an ultrafast laser system described in detail elsewhere,[20] with a 10 kHz repetition rate and ∼100 fs time resolution. For these measurements the excitation wavelength was 400 nm (second harmonic of titanium sapphire) or 530 nm (output of a titanium sapphire pumped optical parametric amplifier, OPA) with a spot size radius of ∼100 μm; longer wavelengths were used for radical states to avoid excitation of residual oxidized flavins. The pulse energy was kept below 400 nJ per pulse. Photoactive proteins were studied in a microflow cell (0.5 mL volume total, 50 μm path length) with CaF_2 windows, which was rastered in the beam path, thus avoiding photobleaching and degradation of the proteins during the measurement. The IR probe transmission was measured as a function of pump−probe delay time after the pump pulse and is reported as TRIR normalized difference spectra [(pump on−pump off)/pump off] at time delays between 1 ps and 2 ns. The pump probe polarization angle was set to magic angle to eliminate any effects of molecular reorientation. The infrared spectra were measured in the ∼1400−1800 cm^{-1} region by two carefully matched 128 pixel MCT detectors, yielding an effective spectral resolution of 3 cm^{-1} per pixel. Wavenumber calibration was relative to the IR transmission of a standard sample of pure *cis*-stilbene placed at the sample position. Proteins were concentrated to 1−1.5 mM before TRIR measurements. For the synthetic radical the concentration was about 1 mM.

Transient Absorption Spectroscopy. Ultrafast transient absorption measurements were performed using a Clark-MXR 1000 regenerative amplifier providing ∼350 μJ pulses centered at 800 nm at a repetition rate of 1 kHz. The output of the amplifier was split in the ratio 1:9. The pulse with the smaller energy was used for generation of the white light continuum probe in a CaF_2 crystal. The higher intensity fraction was either frequency doubled to 400 nm and attenuated to ∼200−400 nJ/pulse before being used as the pump pulse or employed to pump a noncollinear OPA operating at 600 nm, depending on whether oxidized or radical states were to be excited. Polarization of the probe was again set to magic angle. To avoid photodegradation, the samples were moved with the help of a Lissajous scanner and simultaneously flowed by a peristaltic pump. Absorption changes were measured with an Andor CCD and collected with the help of home-written Labview data acquisition software and are again reported as pump on−pump off normalized difference spectra. For these optical experiments sample concentrations were 0.3−0.5 mM.

Density Functional Theory Calculations. Density functional theory (DFT) calculations were performed to assign the measured ground state IR bands of FADH$^\bullet$ and FAD$^{\bullet-}$. The DFT calculations were performed using the Gaussian 03 software package, B3LYP functional, and 6-31G ++ (d,p) basis set.[21] H-bonding effects of the solvent were investigated by adding specific water molecules H-bonded to the C2═O and C4═O carbonyl oxygen atoms (See Figure 1B for atom-numbering scheme). To simulate the experimental data (recorded in D_2O), we exchanged the H atom at the N3 position with D. The calculated frequencies were multiplied by 0.96 (recommended scaling factor for the B3LYP/6-31G calculations[22]) in all cases.

Data Analysis. The measured transient absorbance data $\Delta A(\lambda, t)$ were analyzed using the assumption that ΔA can be written as a sum of a limited number of exponentials

$$\Delta A(\lambda, t) = \sum_i A_i(\lambda)\cdot e^{-k_i t} + C(\lambda)$$

where the k_i are wavelength independent global decay rates, $A_i(\lambda)$ are decay associated spectra (DAS), and $C(\lambda)$ is the so-called final spectrum which is the amplitude extrapolated to $t = \infty$. The values of k_i, $A_i(\lambda)$, and $C(\lambda)$ were calculated by an algorithm written in MATLAB (MathWorks Inc.) based on singular value decomposition.[23] Single wavelength kinetic traces were analyzed by fitting with a sum of exponentials, and the quality of fit gauged by a random residual plot.

dx.doi.org/10.1021/jp2116559 | J. Phys. Chem. B 2012, 116, 5810−5818

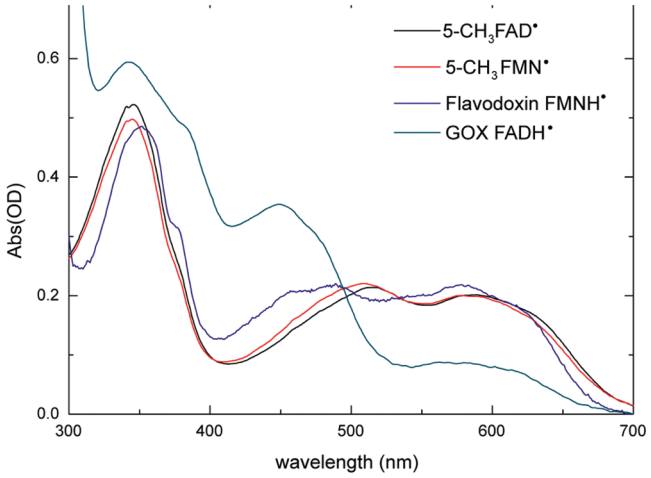

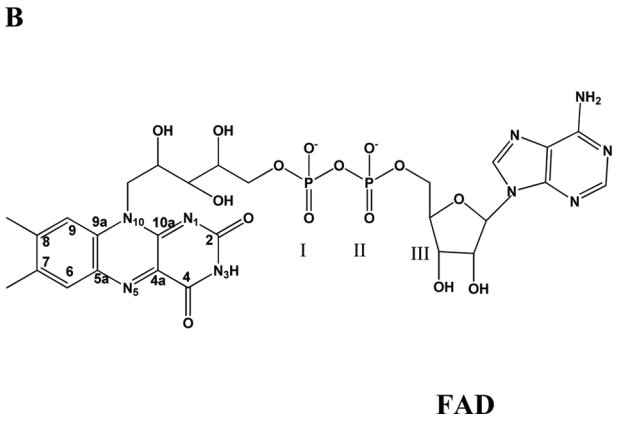

FAD

Figure 1. (A) Absorption spectra of 5-CH_3FAD• and 5-CH_3FMN• in solution, FMNH• in flavodoxin, and FADH• in glucose oxidase (GOX). The spectrum in GOX is a mixture of neutral and radical states. (B) Chemical structure of FAD.

RESULTS AND DISCUSSION

Because flavin radicals are unstable in solution, most measurements on them have been carried out when they are stabilized in proteins[18,24] or reverse micelle environments.[25] However, Eisenberg et al. were able to measure the vibrational resonance Raman spectra of the FMN neutral semiquinone by stabilizing the radical state through attachment of a methyl group at the N5 atom.[17] Following this method we performed measurements on 5-CH_3FAD• and 5-CH_3FMN• neutral semiquinone radicals as model compounds in aqueous solutions using TRIR and visible transient absorption spectroscopy. In order to assess the effect of a protein environment on the radical spectra, the data obtained in solution were compared with measurements in GOX and flavodoxin where the neutral semiquinone (FADH• and FMNH• respectively) was created by photochemical methods. Electronic absorption spectra of methylated neutral flavin radicals in solutions and FADH•/ FMNH• in GOX and flavodoxin are shown in Figure 1A.

Transient Vibrational Spectroscopy of Neutral Flavin Radical. The TRIR spectra of 5-CH_3FAD• and 5-CH_3FMN• (i.e., methylated FADH• and FMNH• radicals) are very similar (Figure 2A), both possessing strong bleaches at 1514, 1528, 1595, and 1628 cm^{-1}. However, the bleach observed in 5-CH_3FMN• at 1664 cm^{-1} was upshifted to ~1675 cm^{-1} and becomes broader and of lower intensity in 5-CH_3FAD•; in general the higher frequency modes appeared slightly broader for 5-CH_3FAD• than 5-CH_3FMN•. The differences between 5-CH_3FAD• and 5-CH_3FMN• suggest some spectral changes due to the interaction between the adenine moiety and the isoalloxazine radical, as is well documented in the fully oxidized state, where FAD is strongly quenched, a result assigned to

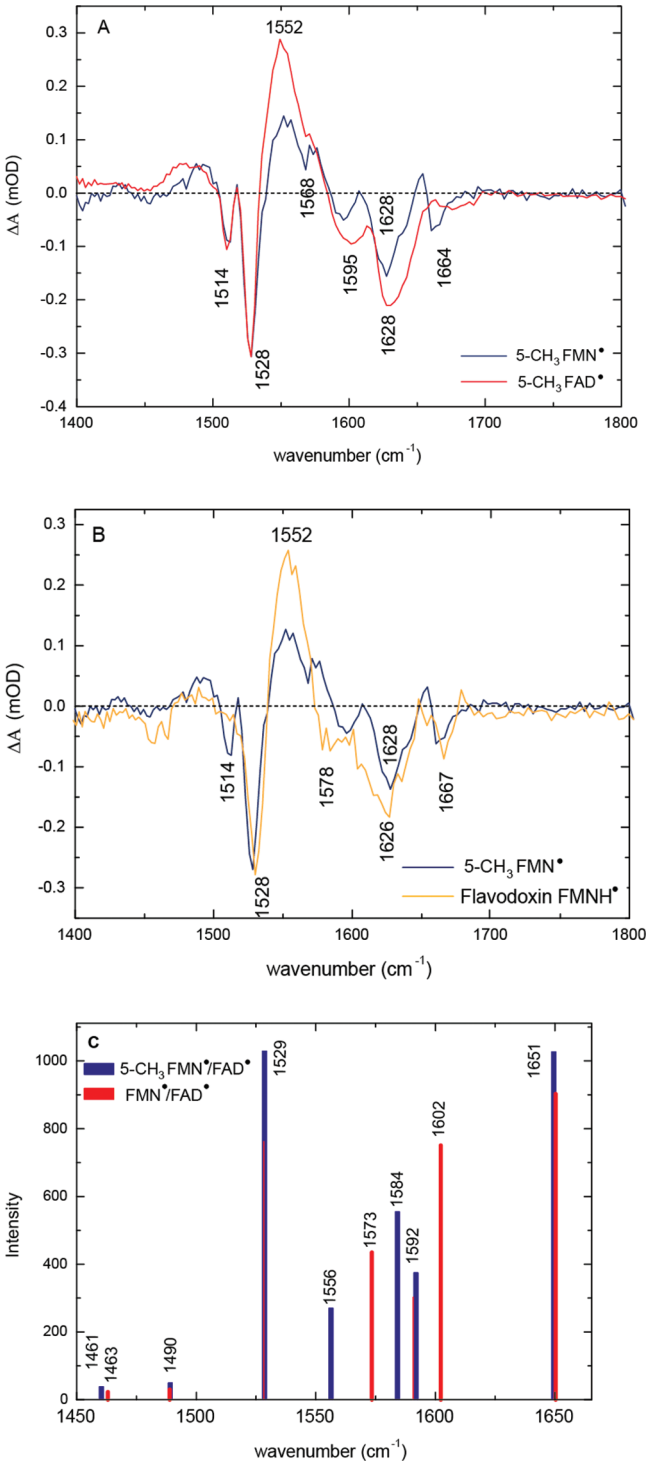

Figure 2. (A) TRIR spectra 5-CH_3FAD• and 5-CH_3FMN• observed at 1 ps delay. Excitation wavelength was set to 530 nm. (B) Comparison of TRIR spectra (observed at 1 ps) of 5-CH_3FMN• in solution and FMNH• in flavodoxin. Excitation wavelength was set to 530 nm. (C) DFT calculations on methylated and nonmethylated lumiflavin neutral radical.

dx.doi.org/10.1021/jp2116559 | J. Phys. Chem. B 2012, 116, 5810–5818

Table 1. Mode Assignments for Methylated Radical

measured/cm^{-1}	1666	1628	1595	1568	1528	1514
DFT/cm^{-1}	1651	1592	1584	1556	1529	1490
assignment	C2═O loc.	C4═O loc.	C═O/ring I	C10aN1/C4aN5	ring	ring

Table 2. Medium Dependence of Vibrational Modes

radical	Raman/TRIR wavenumber/cm^{-1}				
5-CH_3FMN$^\bullet$	1515[a]/1514	1530[a]/1528	1593[a]/1595	1628	1664
5-CH_3FAD$^\bullet$	1516[b]/1514	1528	1590[b]/1595	1628	1670
GOX FADH$^\bullet$		1534[c]/1531		1634 1643	1665
flavodoxin FNM$^\bullet$		1535[d]/1528		1628	1667

[a]Eisenberg et al.[17] [b]Benecky et al.[42] [c]Schelvis et al.[43] [d]Dutta et al.[44]

electron transfer reaction between adenine and the flavin ring.[26−28]

We performed TRIR measurements on flavodoxin when FMN was in its FMNH$^\bullet$ state (Figure 2B). The salient features of flavodoxin stabilized FMNH$^\bullet$ measured at 1 ps are very similar to the 5-CH_3FMN$^\bullet$ spectra: there is a similar ground state bleach at ∼1528 cm^{-1} and excited state absorption at ∼1552 cm^{-1}. The ground state bleach observed at ∼1628 cm^{-1} in 5-CH_3FMN$^\bullet$ is slightly down shifted in the protein, at around 1626 cm^{-1}. These data, in particular the bleach associated with the ground state at 1628 cm^{-1}, will be valuable in characterizing the neutral radical state in the BLUF photocycle.

DFT calculations were performed on unmethylated and 5-methylated lumiflavin to compare with neutral radical states, FMNH$^\bullet$ and 5-CH_3FMN$^\bullet$. To investigate H-bonding interactions, specific water molecules were then included in the calculation, hydrogen bonded to the C2═O and C4═O groups. In lumiflavin the ribityl chain and the adenine groups of FAD and FMN at N10 are replaced by a methyl group, making the calculation more tractable. The calculated frequencies are generally in good agreement with the observed experimental values (Figure 2C, Tables 1 and 2). The highest calculated frequencies, 1651 cm^{-1} in the case of the methylated radical, are associated with the highest experimental frequency, ∼1666 cm^{-1} in both 5-CH_3FMN$^\bullet$ and flavodoxin-FMNH$^\bullet$. This mode involves displacement of the O═C2—N3—C4═O group but is mainly localized on the C2═O stretch. Calculation shows this transition is unaffected by methylation, consistent with experimental observations. The calculated 1592 cm^{-1} transition in the methylated case (1602 cm^{-1} in the nonmethylated case) is associated with the experimentally observed bleach at 1628 cm^{-1} and arises from a mainly C4═O localized stretch which also involves stretching of the O═C2—N3—C4═O groups. We have shown elsewhere that the frequency and character of the flavin carbonyl stretches are sensitive to H-bonding and N3H/D exchange.[12] The H-bonding factor probably accounts for the differences between calculated and observed spectra in this region. For example, the DFT calculations on FADH$^\bullet$ show a marked downshift of the C2═O frequency when specific water molecules H-bonded to the C═O groups are included in the calculation.

The experimentally observed ∼1595 cm^{-1} bleach in the methylated radical and the poorly resolved 1578 cm^{-1} bleach observed in the flavodoxin neutral radical are connected with the calculated 1584 and 1592 cm^{-1} (nonmethylated case) transitions respectively; these modes involve the C4═O carbonyl stretch and an asymmetric stretch of ring I. The calculated 1556 cm^{-1} transition in the methylated radical (1573 cm^{-1} in the nonmethylated case) is associated with the experimental bleach observed at 1568 cm^{-1} in 5-CH_3FMN$^\bullet$ and at 1578 cm^{-1} in flavodoxin-FMNH$^\bullet$. Calculation reveals these to be C10aN1, C4aN5 stretching modes. These negative ΔA (bleach) modes are superimposed on a strong transient absorption. The strong calculated transition at ∼1529 cm^{-1} matches with the experimentally observed value at 1528 cm^{-1} and arises from C−C stretches of the ring I and C4aN5, C10aN1 stretches. The only obvious counterpart of the 1514 cm^{-1} mode observed in the experimental spectra for the methylated compounds is the mode calculated at 1490 cm^{-1} which involves vibrations of essentially the same atoms as the 1529 cm^{-1} mode. The absence of this mode from the spectrum of FMNH$^\bullet$ in flavodoxin deserves comment. The mode is calculated to be present in FMNH$^\bullet$, though weaker (Figure 2C). The DFT calculations show that this mode involves the N5H wag in FMNH$^\bullet$ and is sensitive to H-bonding, being suppressed threefold in intensity by the addition of specific water molecules H-bonded to C2═O and C4═O. We speculate that the disappearance of the 1490 cm^{-1} bleach in flavodoxin reflects the specific H-bond environment of FMNH$^\bullet$. The intense transient absorption around 1552 cm^{-1} arises from the excited state so cannot be assigned from these ground state DFT calculations but is likely to be associated with the carbonyl modes.[29]

In Figure 3A the visible transient absorption spectra of 5-CH_3FAD$^\bullet$ (the 5-CH_3FMN$^\bullet$ spectrum was essentially identical) and GOX-FADH$^\bullet$ are compared. From these transient spectra it is apparent that GOX-FADH$^\bullet$ has an excited state absorption peak at less than 450 nm (it could not be determined exactly as it lies outside of the measurement window), while in the methylated radicals the peak is at approximately 460 nm. The transient spectra in the region of 500−600 nm have the features observed in the linear absorption spectra (Figure 1A). For the methylated radical the two transitions seen in the linear absorption are clearly resolved in the ground state bleach. However, beyond that the broad diffuse nature of the ground and excited state spectra makes them less useful in identifying the flavin radical state in the photocycle than the vibrational spectra (Figure 2).

Kinetics of Neutral Flavin Radical. The kinetics of 5-CH_3FAD$^\bullet$ and 5-CH_3FMN$^\bullet$ radicals in D_2O are essentially the same, with a ground recovery time of 13 ± 0.5 ps measured by visible transient absorption experiments (Figure 3B). Evidently the adenine moiety plays no role in the excited state decay of the radical state. A similar value 11 ± 2 ps was observed for the decay of the excited state absorption measured by transient

dx.doi.org/10.1021/jp2116559 | J. Phys. Chem. B 2012, 116, 5810−5818

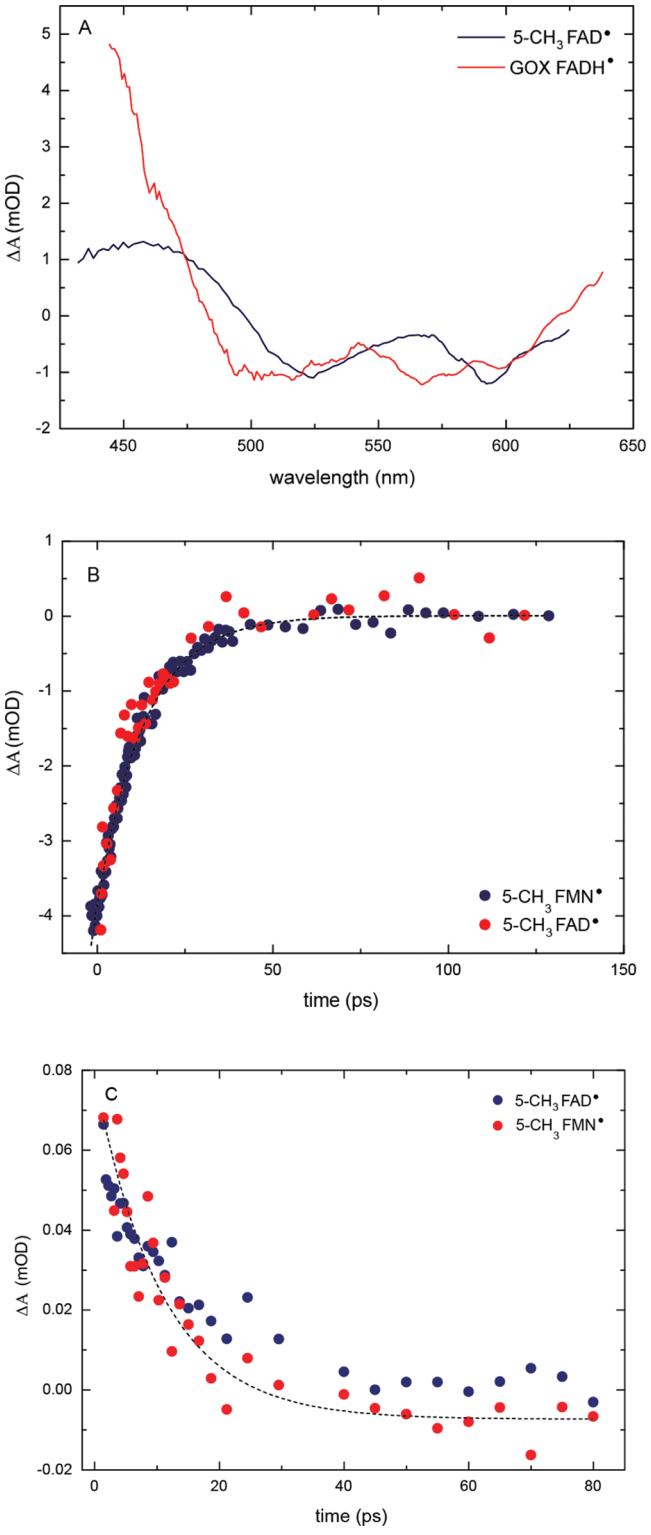

Figure 3. (A) Visible transient absorption spectra of 5-CH_3FAD$^\bullet$ in solution and FADH$^\bullet$ in GOX at 3 ps after excitation. Methylated radical spectra were obtained with excitation at either 530 or 600 nm and the respective spectra stitched together, thus avoiding gaps due to scattered excitation light. The spectra are normalized to the bleach of the GOX sample. (B) Ground state recovery of 5-CH_3FAD$^\bullet$ and 5-CH_3FMN$^\bullet$ in solution measured at 525 nm. Dotted line is the monoexponential fit of the 5-CH_3FAD$^\bullet$ recovery. (C) Excited state decay of 5-CH_3FAD$^\bullet$ and 5-CH_3FMN$^\bullet$ in solution at 1552 cm^{-1}. Excitation wavelength was set to 530 nm.

infrared at 1552 cm^{-1} (Figure 3C). The close agreement of these results confirms that the radiationless decay mechanism in the radical states is internal conversion from S_1 to S_0.

The excited state kinetics of the flavin cofactor observed in flavodoxin and GOX show significant differences to those measured in solution. In Figure 4 A and B the excited state decay times for the methylated radicals in solution are compared with measurements of both the neutral radical state and the oxidized state of flavin bound to flavodoxin (Figure 4A) and GOX (Figure 4B). The most striking result is that in flavodoxin the decay time for both oxidized and radical states is faster than for the radical in solution, while for GOX the oxidized FAD decay time is faster, but for the radical state it is slower, than for the radical in solution. Evidently the protein binding site has a major effect on the decay kinetics.

The excited state kinetics of oxidized FMN in flavodoxin were measured earlier by Mataga and co-workers using time-resolved fluorescence up-conversion.[30] They found that the decay was dominated by an ultrafast component of 158 fs. Our

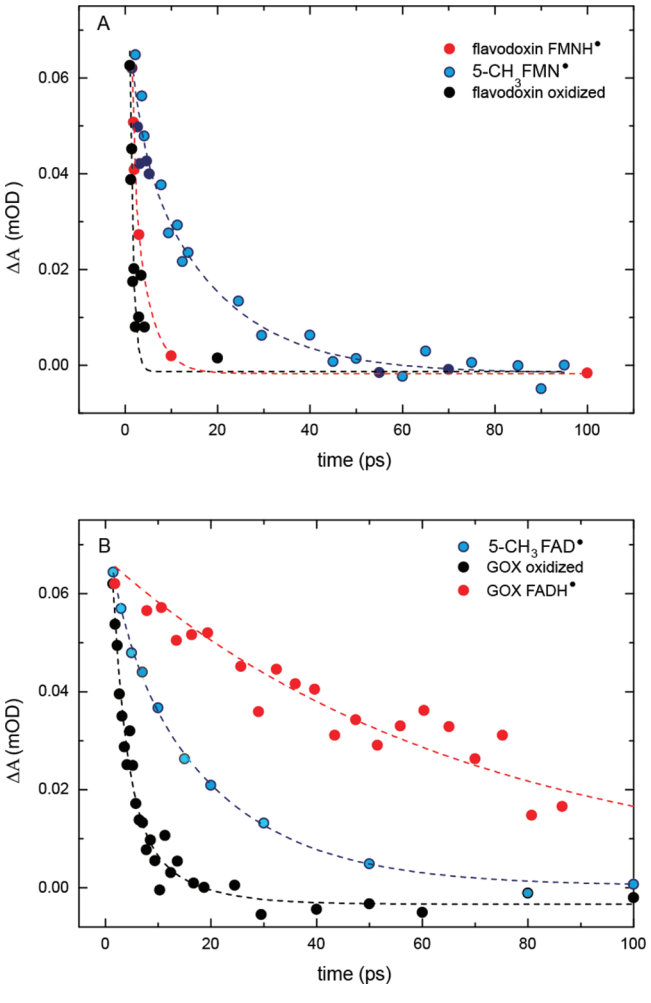

Figure 4. Excited state decay of (A) flavodoxin with FMN oxidized (excited at 400 nm) at 1561 cm^{-1}, FMNH$^\bullet$ (excited at 530 nm), and 5-CH_3FMN$^\bullet$ at 1552 cm^{-1} (excited at 530 nm); (B) glucose oxidase with FAD oxidized (excited at 400 nm) at 1571 cm^{-1}, FADH$^\bullet$ (excited at 530 nm), and 5-CH_3FAD$^\bullet$ at 1552 cm^{-1} (excited at 530 nm). Colored dash lines are monoexponential fits to the respective measurements (data are normalized to the change in absorbance of the model compound).

dx.doi.org/10.1021/jp2116559 | J. Phys. Chem. B 2012, 116, 5810–5818

TRIR measurement at 1561 cm^{-1} on oxidized flavodoxin reveal a <500 fs decay time; given the signal-to-noise achieved in the TRIR data and the low concentration of the sample, the present data can be regarded as being in agreement with the fluorescence data, i.e., that there is an ultrafast, sub-500 fs excited state decay of the oxidized state of FMN in flavodoxin. This decay was assigned to quenching by electron transfer from tryptophan and/or tyrosine to FMN, as the isoalloxazine ring is sandwiched between a tryptophan and tyrosine residue.

Excited state decay of flavodoxin-FMNH• was also measured earlier by Vos and co-workers using visible transient absorption spectroscopy.[18] They measured the excited state decay as 2.3 ± 0.3 ps at 700 nm. Again the TRIR measurement is in good agreement with these data; the decay observed at 1553 cm^{-1} was fit with a single exponential and found to have a decay constant of 1.7 ± 0.3 ps. This relaxation time is faster than reported in the transient fluorescence measurements of Kao et al., who studied the W60F/Y98F mutant of flavodoxin, a result which is consistent with a role for these residues in electron transfer quenching.[31]

The difference observed in the rate of the primary electron donor transfer step in the case of the oxidized and semiquinone states has been discussed previously by Pan et al.[18] In both cases an electron transfer was suggested as the quenching mechanism, with the difference in rates reflecting the different redox potentials of oxidized and semiquinone states. However, no products of the electron transfer reaction were observed. The oxidation state dependence of the electron transfer rate may be related to the hydrogen bonding at N5 of the isoalloxazine ring. In the semiquinone state a protein conformational change compared to the oxidized state is observed, resulting in the formation of a hydrogen bond between the N5 hydrogen of the isoalloxazine ring and the carbonyl oxygen of G61.[32] The alteration of the hydrogen bonding to the N5 hydrogen may be a factor modulating the redox potential of the flavin in a manner which slows the reaction compared to the oxidized state.

The time constant for the excited state decay of FADH• in GOX measured here by TRIR at 1550 cm^{-1} was 67 ± 6 ps which is close to the 59 ± 5 ps value measured by Vos and co-workers using visible transient absorption.[18] This is much slower than for 5-CH_3FAD•and 5-CH_3FMN• in solution (Figure 4B). Since there is no electron donor available in the solution to quench the excited state, the reduced quenching in GOX must correspond to suppression of the radiationless decay by the protein. It is proposed that the radiationless decay by internal conversion is promoted by motion along a coordinate which is sensitive either to the H-bonding environment or to excited state structural reorganization, as has been discussed for the fully reduced states.[16,31] The longer decay time in GOX could thus be ascribed to restriction of this motion in the rigid (H-bonded) protein environment.

The kinetics of oxidized FAD in GOX are ultrafast and heterogeneous. The excited state decay measured at the 1611 cm^{-1} transient absorption (Figure 5A) was fit with a monoexponential function with a 3 ± 0.3 ps component, while the ground state recovery (at 1550 cm^{-1}) can be fit with two exponentials, the recovery times being 3.2 ± 0.2 and 26 ± 3 ps (data shown in the Supporting Information); these picosecond kinetics are broadly in agreement with earlier measurements.[32] Again the quenching mechanism was assigned to electron transfer from tryptophan or tyrosine to the excited FAD. This assignment is supported by agreement with detailed

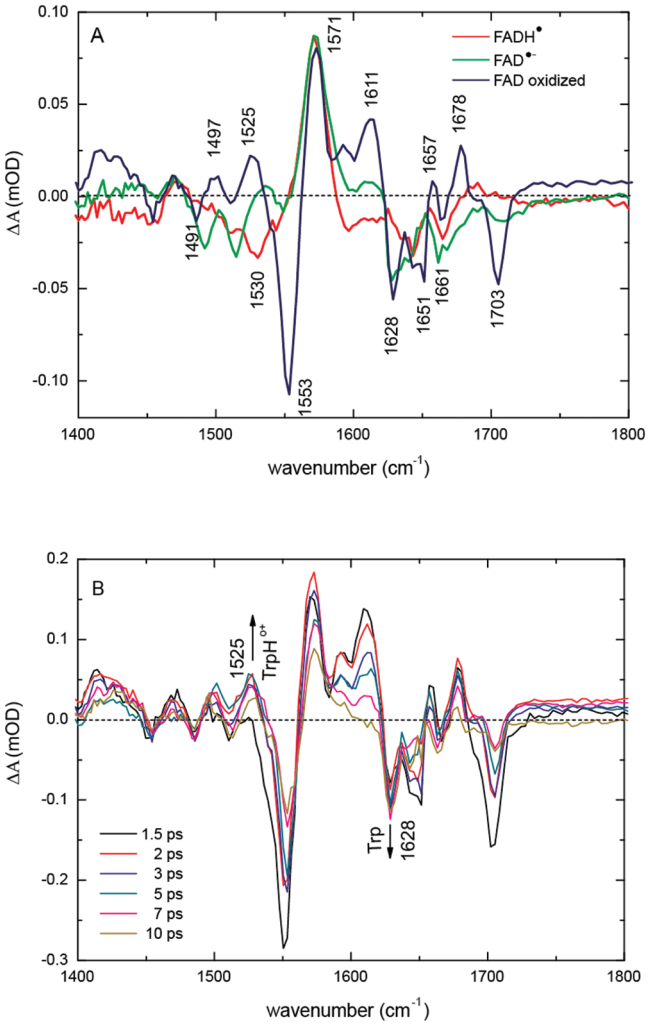

Figure 5. (A) TRIR spectra at 1.5 ps delay for GOX in which the flavin cofactor is oxidized FAD, FADH•, and FAD•⁻ states, respectively. (B) TRIR spectra of oxidized GOX at different delay times from 1.5 to 10 ps.

theoretical calculations of the electron transfer rate.[33] However, such calculations require some assumptions concerning redox potentials and the protein matrix. To investigate this mechanism further, we performed TRIR measurements on GOX with the flavin cofactor in three different redox states: oxidized, neutral radical, and anionic radical.

The spectrum of the oxidized GOX (Figure 5A) at early times after excitation is very similar to the spectrum of oxidized FAD.[12,34] The major ground state bleaches at 1553, 1651, and 1703 cm^{-1} have been assigned to mainly C10aN1, C_2═O, and C_4═O localized vibrations of the isoalloxazine ring, respectively through DFT calculation and isotope substitution.[12,34,35] In general the vibrational bands in the protein are somewhat narrower than in solution, suggesting a more ordered environment.

The spectra of GOX with the flavin cofactor in its anionic radical and neutral radical states recorded 1.5 ps after excitation are also shown in Figure 5A. The FADH• spectrum is very similar to the spectrum observed in the methylated radical (Figure 2) except that the strong excited state absorption is shifted to ~1571 cm^{-1}. The absence of the prominent 1628 cm^{-1} peak and the appearance of a peak at ~1640 cm^{-1} may be artifacts of the measurement as the very strong infrared

dx.doi.org/10.1021/jp2116559 | J. Phys. Chem. B 2012, 116, 5810–5818

absorption of the GOX backbone in this spectral region makes the calculation of ΔA uncertain. The measured TRIR data also show that there are only small differences between the $FAD^{\bullet-}$ and $FADH^{\bullet}$ spectra in GOX: $FAD^{\bullet-}$ has a more prominent ~1514 cm^{-1} peak and an additional peak at 1491 cm^{-1}. Since the chromophore is the same in both cases it is likely that this additional feature is associated with a protein mode coupled to the excitation. A much stronger example of such protein—chromophore coupling in a flavoprotein was reported in our recent study of the Q63E AppA mutant.[36] The $FAD^{\bullet-}$ IR vibrational data for the ground electronic state are reflected in the main bleach modes. The observed frequencies are in good agreement with the resonance Raman spectrum of the GOX $FAD^{\bullet-}$ state measured previously:[37] the Raman spectrum contains strong peaks at 1514, 1553, 1578, 1623, and 1670 cm^{-1}.

In Figure 5B the time dependent TRIR spectra for oxidized FAD in GOX are shown. If, as reported, the quenching mechanism arises from an electron transfer reaction, some time dependent features associated with the formation of radical states are expected in the TRIR spectrum. Many of the strong bleach features appear within the duration of the pulses and are close to the spectra of FAD. They can thus be assigned to the oxidized FAD ground state, which recovers on the tens of picoseconds time scale. Somewhat faster kinetics are evident between 1550 and 1650 cm^{-1}. The disappearance of the band near 1610 cm^{-1} on a time scale faster than the ground state recovery is indicative of a reactive species. Similarly the bleach at 1628 cm^{-1} becomes stronger as the other bleach modes recover, consistent with loss of ground state by reaction. There is thus clear evidence in Figure 5B for an excited state reaction.

In order to analyze the TRIR measurements quantitatively, we performed a global analysis on the oxidized GOX data. The global fit was best when two exponentials with the values of 2.5 and 26 ps were included in the analysis. The decay associated spectrum (Figure 6) assigned to the 2.5 ps component is similar to spectra at early times, the main difference being the appearance of an intense transient peak at ~1628 cm^{-1}. The 2.5 ps kinetics are close to the main component of the quenching time reported in time-resolved fluorescence and are associated with the electron transfer reaction.[32] The rapidly decaying 1628 cm^{-1} mode may thus be due to a vibrational mode associated with a reaction partner, for example, tryptophan; transitions at similar wavenumber are observed in the ground state IR of tryptophan containing peptides.[38] The DAS belonging to the 26 ps component can be described as a mixture of the GOX oxidized and GOX-$FAD^{\bullet-}$ state: as one can see from Figure 6 the 1550 cm^{-1} peak belongs to the oxidized state but it is not as prominent as observed in the oxidized case; the 1611 cm^{-1} transient and the bleach observed at 1703 cm^{-1} are stronger than in $FAD^{\bullet-}$. This is in agreement with the assumption that after photoexcitation the flavin cofactor of GOX is reduced, forming the $FAD^{\bullet-}$ state. The differences between the decay associated spectra of the slower phase and the $FAD^{\bullet-}$ spectra are possibly connected to the appearance of the tryptophan radical cation $TrpH^{\bullet+}$.

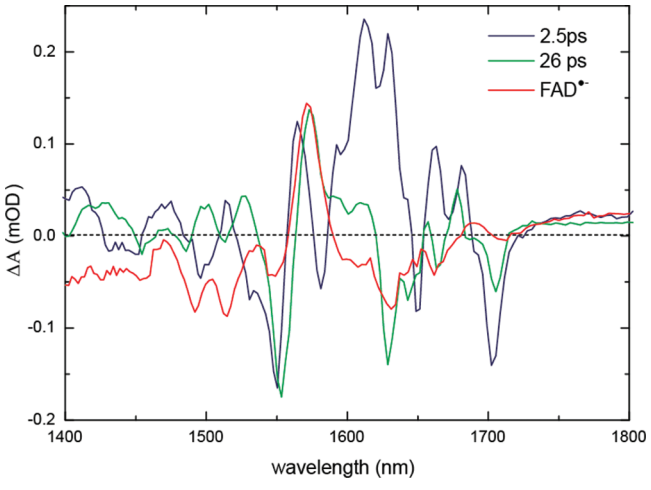

Figure 6. Decay associated spectra of oxidized GOX recovered from a global fit.

Analyzing the visible transient absorption data measured for oxidized GOX (Figure 7) aids the spectral assignment of the

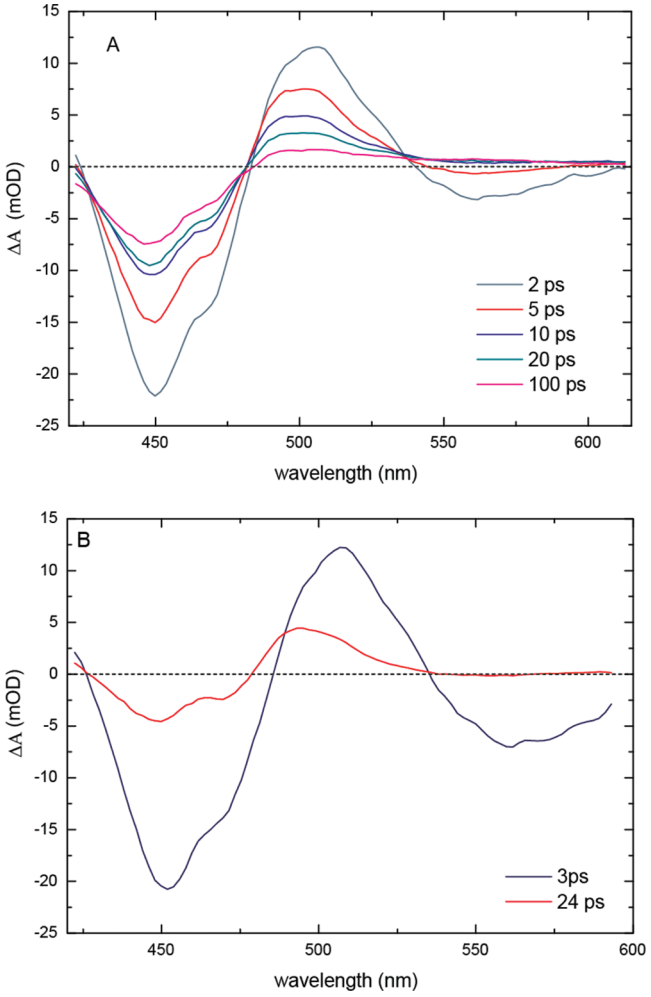

Figure 7. (A) Transient absorption spectra of oxidized GOX at different time delays. (B) Decay associated spectra of oxidized GOX (3 and 24 ps).

two DAS observed in the TRIR data. The global analysis of the transient electronic spectra (Figure 7B) resulted in two very similar time components (2.5, 26 ps) to the TRIR data. The fast (2.5 ps) component can be associated with the usual oxidized FAD spectrum. The slower (26 ps) component is less readily assigned, but it can be very approximately modeled as $(FAD^{\bullet-} + TrpH^{\bullet+}) - (FAD_{ox} - Trp)$;[5] although this is not

dx.doi.org/10.1021/jp2116559 | J. Phys. Chem. B 2012, 116, 5810–5818

definitive, it is consistent with the TRIR data; these data are shown in the Supporting Information.

Analysis of the TRIR kinetics at individual wavenumbers adds further detail to this picture. Based on the experimental data measured on the GOX-FAD$^{\bullet-}$ at 1628 cm^{-1}, a positive peak forming after photoexcitation would be predicted, but instead of this a fast decay (3 ± 0.5 ps) of the absorption change and a slower (26 ± 3 ps) recovery (Figure 8A) are

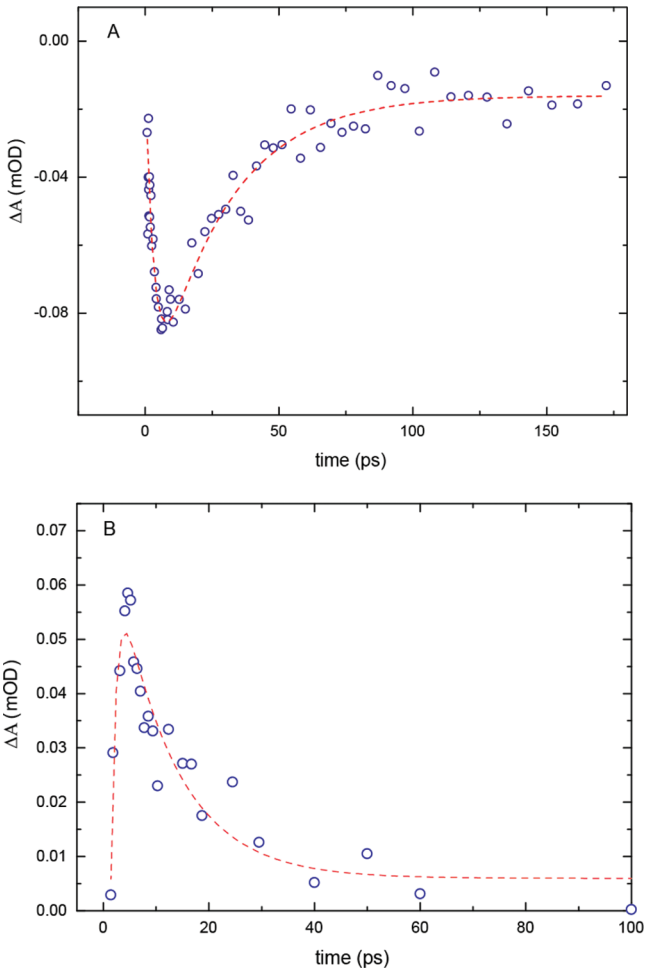

Figure 8. (A) Kinetics of oxidized GOX observed at 1628 cm^{-1}. (B) Kinetics of oxidized GOX observed at 1525 cm^{-1} (fitted lines in red).

observed. A plausible explanation for this behavior is that the fast decay of the absorption change is due to protonation of an aromatic residue which served as the electron donor to FAD. The disappearance of the absorption of an aromatic residue (Trp/Tyr) results in the increasingly negative value in the difference spectra. Similar kinetics were reported by Fujiwara and Mizutani[39] in their time-resolved ultraviolet resonance Raman measurements (UVRR); a transient species was observed at 1625 cm^{-1} which was assigned to an FAD$^{\bullet-}$ + TrpH$^{\bullet+}$ peak.[39] Analyzing the kinetics measured at 1525 cm^{-1} (Figure 5B and Figure 8B) reveals that a new state is formed within ~1.5 ps. Based on earlier UVRR measurements[40] of the TrpH$^{\bullet+}$ spectrum in aqueous solution, the observed kinetics may plausibly be assigned to the formation of TrpH$^{\bullet+}$. The appearance of the TrpH$^{\bullet+}$ is further supported by the appearance of the transient at 1497 cm^{-1} (Figure 5A) recently assigned by Vlcek and co-workers as a marker for the TrpH$^{\bullet+}$.[41]

CONCLUSIONS

The photophysical properties of N5-methyl FAD and N5-methyl FMN radicals in solution were characterized by means of ultrafast transient visible and infrared spectroscopy. The bleach transitions were assigned with the aid of DFT calculations. It was found that the excited state lifetime of these methylated flavin radicals in aqueous solution is ~13 ps and that the decay mechanism is internal conversion. The transient infrared spectra of flavodoxin and GOX were also measured when the flavin cofactor was in its neutral radical state. It was found that the decay kinetics are a sensitive function of the protein binding site, a fact that could be ascribed to electron transfer quenching reactions and environment dependent suppression of internal conversion.

The photodynamics of the flavoprotein GOX were examined in detail in three oxidation states through visible and IR measurements. By means of global analysis and individual wavenumber fitting, the formation of the anionic radical state of the flavin cofactor in GOX was characterized and the formation of the TrpH$^{\bullet+}$ was proposed. In addition to confirming the mechanism of FAD quenching in GOX, these data yield transient IR spectra which will be vital in the characterization of the BLUF domain photocycle. Further TRIR experiments on AppA and its mutants are currently under analysis.

ASSOCIATED CONTENT

Supporting Information

Additional data on the chemical synthesis, the kinetics of oxidized GOX, and modeling of the decay associated spectra. This material is available free of charge via the Internet at http://pubs.acs.org.

AUTHOR INFORMATION

Corresponding Author

*E-mail: s.meech@uea.ac.uk (S.R.M.); ptonge@notes.cc.sunysb.edu (P.J.T.).

Notes

The authors declare no competing financial interest.

ACKNOWLEDGMENTS

We thank Dr. Corinne Aubert for providing Flavodoxin from *Desulfovibrio gigas*. We are grateful to EPSRC EP/G002916 and NSF CHE-0822587 for financial support to S.R.M. and P.J.T., respectively, and to STFC for programme access to the ULTRA (TRIR) facility.

REFERENCES

(1) Massey, V. *Biochem. Soc. Trans.* **2000**, *28*, 283−296.
(2) Losi, A.; Gartner, W. *Photochem. Photobiol.* **2010**, *87*, 491−510.
(3) Aubert, C.; Vos, M. H.; Mathis, P.; Eker, A. P. M; Brettel, K. *Nature* **2000**, *405*, 586−590.
(4) Lukacs, A.; Eker, A. P. M; Byrdin, M.; Brettel, K.; Vos, M. H. *J. Am. Chem. Soc.* **2008**, *130*, 14394−14395.
(5) Brazard, J.; Usman, A.; Lacombat, F.; Ley, C.; Martin, M. M.; Plaza, P.; Mony, L.; Heijde, M.; Zabulon, G.; Bowler, C. *J. Am. Chem. Soc.* **2010**, *132*, 4935−4945.
(6) Biskup, T.; Schleicher, E.; Okafuji, A.; Link, G.; Hitomi, K.; Getzoff, E. D.; Weber, S. *Angew. Chem., Int. Ed.* **2009**, *48*, 404−407.
(7) Anderson, S.; Dragnea, V.; Masuda, S.; Ybe, J.; Moffat, K.; Bauer, C. *Biochemistry* **2005**, *44*, 7998−8005.
(8) Masuda, S.; Bauer, C. E. *Cell* **2002**, *110*, 613−623.
(9) Unno, M.; Sano, R.; Masuda, S.; Ono, T. A.; Yamauchi, S. *J. Phys. Chem. B* **2005**, *109*, 12620−12626.

(10) Alexandre, M. T. A.; van Wilderen, L. J. G.; van Grondelle, R.; Hellingwerf, K. J.; Groot, M. L.; Kennis, J. T. M. *Biophys. J.* **2005**, *88*, 509A−509A.
(11) Gauden, M.; Yeremenko, S.; Laan, W.; van Stokkum, I. H. M.; Ihalainen, J. A.; van Grondelle, R.; Hellingwerf, K. J.; Kennis, J. T. M. *Biochemistry* **2005**, *44*, 3653−3662.
(12) Haigney, A.; Lukacs, A.; Zhao, R. K.; Stelling, A. L.; Brust, R.; Kim, R. R.; Kondo, M.; Clark, I.; Towrie, M.; Greetham, G. M.; et al. *Biochemistry* **2011**, *50*, 1321−1328.
(13) Stelling, A. L.; Ronayne, K. L.; Nappa, J.; Tonge, P. J.; Meech, S. R. *J. Am. Chem. Soc.* **2007**, *129*, 15556−15564.
(14) Bonetti, C.; Mathes, T.; van Stokkum, I. H. M.; Mullen, K. M.; Groot, M. L.; van Grondelle, R.; Hegemann, P.; Kennis, J. T. M. *Biophys. J.* **2008**, *95*, 4790−4802.
(15) Jung, A.; Domratcheva, T.; Tarutina, M.; Wu, Q.; Ko, W. H.; Shoeman, R. L.; Gomelsky, M.; Gardner, K. H.; Schlichting, L. *Proc. Natl. Acad. Sci. U.S.A.* **2005**, *102*, 12350−12355.
(16) Zhao, R.-K.; Lukacs, A.; Haigney, A.; Brust, R.; Greetham, G. M.; Towrie, M.; Tonge, P. J.; Meech, S. R. *Phys. Chem. Chem. Phys.* **2011**, *13*, 17642−17648.
(17) Eisenberg, A. S.; Schelvis, J. P. M *J. Phys. Chem. A* **2008**, *112*, 6179−6189.
(18) Pan, J.; Byrdin, M.; Aubert, C.; Eker, A. P. M; Brettel, K.; Vos, M. H. *J. Phys. Chem. B* **2004**, *108*, 10160−10167.
(19) Massey, V.; Stankovich, M.; Hemmerich, P. *Biochemistry* **1978**, *17*, 1−8.
(20) Greetham, G. M.; Burgos, P.; Cao, Q. A.; Clark, I. P.; Codd, P. S.; Farrow, R. C.; George, M. W.; Kogimtzis, M.; Matousek, P.; Parker, A. W.; Pollard, M. R.; Robinson, D. A.; Xin, Z. J.; Towrie, M. *Appl. Spectrosc.* **2010**, *64*, 1311−1319.
(21) Frisch, M. J.; Trucks, G. W.; Schlegel, H. B.; Scuseria, G. E.; Robb, M. A.; Cheeseman, J. R.; Montgomery, J. A., Jr.; Vreven, T.; Kudin, K. N.; Burant, J. C.; Millam, J. M.; et al. *Gaussian 03*, revision A.1; Gaussian, Inc.: Pittsburgh, PA, 2003.
(22) Scott, A. P.; Radom, L. *J. Phys. Chem.* **1996**, *100*, 16502−16513.
(23) Liebl, U.; Lambry, J. C.; Leibl, W.; Breton, J.; Martin, J. L.; Vos, M. H. *Biochemistry* **1996**, *35*, 9925−34.
(24) Massey, V.; Palmer, G. *Biochemistry* **1966**, *5*, 3181−3189.
(25) Kurreck, H.; Bretz, N. H.; Helle, N.; Henzel, N.; Weilbacher, E. *J. Chem. Soc., Faraday Trans. 1* **1988**, *84*, 3293−3306.
(26) Chosrowjan, H.; Taniguchi, S.; Mataga, N.; Tanaka, F.; Visser, A. *Chem. Phys. Lett.* **2003**, *378*, 354−358.
(27) Li, G.; Glusac, K. D. *J. Phys. Chem. B* **2008**, *112*, 10758−10764.
(28) van den Berg, P. A. W.; van Hoek, A.; Walentas, C. D.; Perham, R. N.; Visser, A. *Biophys. J.* **1998**, *74*, 2046−2058.
(29) Wolf, M. M.; Schumann, C.; Gross, R.; Domratcheva, T.; Diller, R. *J. Phys. Chem. B* **2008**, *112*, 13424−13432.
(30) Mataga, N.; Chosrowjan, H.; Taniguchi, S.; Tanaka, F.; Kido, N.; Kitamura, M. *J. Phys. Chem. B* **2002**, *106*, 8917−8920.
(31) Kao, Y. T.; Saxena, C.; He, T. F.; Guo, L. J.; Wang, L. J.; Sancar, A.; Zhong, D. P. *J. Am. Chem. Soc.* **2008**, *130*, 13132−13139.
(32) Zhong, D. P.; Zewail, A. H. *Proc. Natl. Acad. Sci. U.S.A.* **2001**, *98*, 11867−11872.
(33) Tanaka, F.; Rujkorakarn, R.; Chosrowjan, H.; Taniguchi, S.; Mataga, N. *Chem. Phys.* **2008**, *348*, 237−241.
(34) Kondo, M.; Nappa, J.; Ronayne, K. L.; Stelling, A. L.; Tonge, P. J.; Meech, S. R. *J. Phys. Chem. B* **2006**, *110*, 20107−20110.
(35) Wolf, M. M. N.; Schumann, C.; Gross, R.; Domratcheva, T.; Diller, R. *J. Phy. Chem. B* **2008**, *112*, 13424−13432.
(36) Lukacs, A.; Haigney, A.; Brust, R.; Zhao, R.-K.; Stelling, A. L.; Clark, I. P.; Towrie, M.; Greetham, G. M.; Meech, S. R.; Tonge, P. J. *J. Am. Chem. Soc.* **2011**, *133*, 16893−16900.
(37) Zhelyaskov, V. R.; Bhattacharyya, A. K.; Edmondson, D. E.; Yue, K. T. *FASEB J.* **1992**, *6*, A319−A319.
(38) Bagchi, S.; Kim, Y. S.; Charnley, A. K.; Smith, A. B.; Hochstrasser, R. M. *J. Phys. Chem. B* **2007**, *111*, 3010−3018.
(39) Mizutani, Y.; Fujiwara, A. *J. Raman Spectrosc.* **2008**, *39*, 1600−1605.
(40) Johnson, C. R.; Ludwig, M.; Asher, S. A. *J. Am. Chem. Soc.* **1986**, *108*, 905−912.
(41) Blanco-Rodriguez, A. M.; Towrie, M.; Sykora, J.; Zalis, S.; Vlcek, A. *Inorg. Chem.* **2011**, *50*, 6122−6134.
(42) Benecky, M. J.; Copeland, R. A.; Spiro, T. G. *Biochim. Biophys. Acta* **1983**, *760*, 163−168.
(43) Schelvis, J. P. M; Pun, D.; Goyal, N.; Sokolova, O. *J. Raman. Spectrosc.* **2006**, *37*, 822−829.
(44) Dutta, P. K.; Spiro, T. G. *Biochemistry* **1980**, *19*, 1590−1593.